Design of Inner Baffle Array for Compact Multi-Aperture Off-Axis Optical System

Peixian Han[1,2,3,4], Junli Guo[1,2,3,4], Meili Zhang[1,4], Bingxu Chen[1,4], Ge Ren[1,2,3,4,*] and Yong Liu[2]
[1]*Key Laboratory of Optical Engineering, Chinese Academy of Sciences, Chengdu 610209, China*
[2]*School of Optoelectronic Science and Engineering, University of Electronic Science and Technology of China, Chengdu 611731, China*
[3]*University of Chinese Academy of Sciences, Beijing 100039, China*
[4]*Institute of Optics and Electronics, Chinese Academy of Sciences, Chengdu 610209, China*

Keywords: Multi-Aperture Optical System, Stray Light Analysis, BRDF Measurement, Inner Baffle Array Design.

Abstract: In order to realize the light and miniaturization of the imaging telescope of the optical communication system, a design method of the inner baffle array of the compact multi-aperture off-axis beam transmission system is developed in this paper. This method mainly deduces the inclination angle of the inclined section of the inner baffle of the multi-aperture off-axis beam transmission system by the method of spatial analytic geometry, and establishes a compact three-aperture inner baffle array in the off-axis beam transmission system by using 3D modeling software. The bidirectional reflection distribution function (BRDF) of inorganic oxidized Al/SiC, oxidized TC4, untreated carbon fiber reinforced plastic (CFRP), and indene steel was tested by the angular determination scatterometer, and the scattering data of CFRP with the highest cost performance was put into the stray light analysis software to simulate the point source transmittance (PST) of the inclined section and the flush section of the baffle tube array. The simulation results show that the proposed method can effectively improve the cross-talk of external stray light between the sub-aperture of the multi-aperture off-axis beam transmission system.

1 INTRODUCTION

Optical communication has the advantages of high speed, low power consumption and high security, which is an effective means to achieve satellite-ground big data communication in the future. After reaching the receiving plane, the signal light emitted by the traditional single-aperture imaging system is severely distorted, and the energy concentration is low. Using beam synthesis (coherent synthesis or incoherent synthesis) method to combine multiple beams to realize beam array multi-aperture transmission system is an important way to effectively overcome the nonlinear effect of beam gain medium, overcome the influence of atmospheric turbulence phase, and obtain higher power. Space systems have strict restrictions on volume and weight, so compact, light and miniaturization are the development trends of space systems. The compact multi-aperture optical communication system can reduce the size of the system structure, reduce the cost of the system, and improve the cost performance of the system while obtaining high power and maintaining good beam quality.

Stray light refers to the light that diffuses outside the imaging light in the optical system on the surface of the detector, and the light that reaches the detector by abnormal optical path. During imaging, the system must have a strong ability to exclude stray light, otherwise sunlight or other stray light sources will sink the imaging beam. If the stray light is not properly eliminated, it may result in a false response or noise flooding the real light signal due to the low illuminance and large dynamic range of targets. At the same time, the space target detection camera working outside the atmosphere would inevitably be disturbed by the sunlight, the moon, the ground light, the outer surface of spacecraft and the scattering of components, resulting in an increase in the image surface stray light gray scale, and the image surface illumination distribution was not uniform, which

*Corresponding author: renge@ioe.ac.cn

Han, P., Guo, J., Zhang, M., Chen, B., Ren, G. and Liu, Y.
Design of Inner Baffle Array for Compact Multi-Aperture Off-Axis Optical System.
DOI: 10.5220/0011665200003408
In *Proceedings of the 11th International Conference on Photonics, Optics and Laser Technology (PHOTOPTICS 2023)*, pages 52-58
ISBN: 978-989-758-632-3; ISSN: 2184-4364

affected the improvement of signal-to-noise ratio and the identification of debris.

Compact multiple aperture off-axis imaging system between each sub aperture has the problem of crosstalk of stray light outside the field of view. The traditional inner baffle array with flush section has poor suppression effect on the out-of-field stray light from adjacent sub-aperture. The stray light outside the field of view of adjacent aperture will pass through the inner baffle and enter the subsequent imaging optical path, and there is light leakage phenomenon. In this paper, in view of the phenomenon that the stray light outside the field of view between the sub apertures of the compact multi-aperture off-axis imaging system crosstalk with each other, a new design method for the inner baffle array is invented, taking a set of three aperture compact off-axis beam narrowing system as an example, which successfully prevents the stray light lines outside the field of view from adjacent apertures from passing through the inner baffle and entering the subsequent imaging optical path.

2 OPTICAL SYSTEM STRUCTURE

The compact multi-aperture optical communication system consists of three main optical systems and subsequent optical systems. The main optical system adopts the afocal Mersenne-Cassegrain design, which is conducive to the assembly of the system and the optical path docking between various subsystems after the disassembly and assembly of the whole machine. Both the primary mirror (PM) and the secondary mirror (SM) are off-axis paraboloids, forming an off-axis afocal-beam, which can reduce the difficulty of detection and processing of large-diameter PM and convex SM. The optical structure layout of a single aperture is shown in Figure 1. The structure layout of the three-aperture optical system is shown in Figure 2.

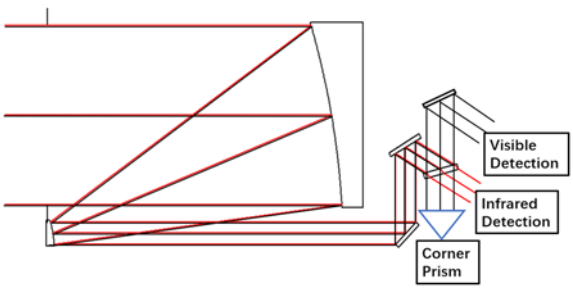

Figure 1: Schematic optics layout of the common optical path design.

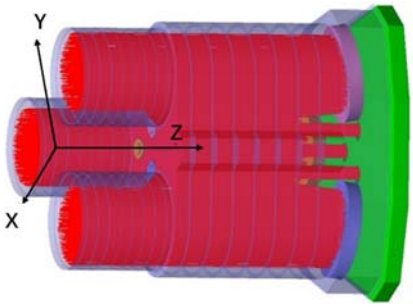

Figure 2: The structure layout of the three-aperture imaging system.

3 MODEL GEOMETRY DESIGN AND VERIFICATION

3.1 The Two-Stage Fore Baffle Design

Baffles are employed to eliminate the direct light that can reach the detector without any scattering. For a two-mirror optical system, the most common baffles are external baffle and the internal baffles near the mirrors. The design principle of the conventional baffle of coaxial two-mirror optical system is shown in Figure 3. To ensure that all the imaging beams enter the optical system, the outer baffle should be at an angle of ω, equal to half of the FOV, in relation to the optical axis. In Figure 3, the edges of the PM and SM baffle are points B and A, respectively. If points A and B are connected and extended, the intersection point of line AB and the fore baffle is point E. However, the slope of line A'B' in the off-axis two-mirror beam- narrowing system is small, which leads to the excessive length of the fore baffle.

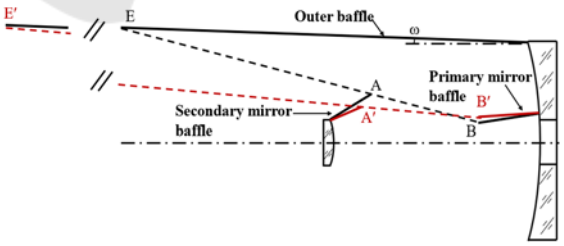

Figure 3: The design principle of the conventional baffle of coaxial two-mirror optical system.

Adding the built-in baffle to the optical path will affect the beam quality of the transmitted beam and affect the imaging efficiency. Therefore, a more reliable method to reduce the system baffle length is needed. As shown in Figure 4, an entrance baffle is added at the front end of each separate beam transmission system to block out of field stray light

greater than 45 °. A single beam transmission system is combined into a whole through an outer envelope primary lens cone between the primary and secondary mirrors of the system, which is used to reduce the total weight and the volume of the apparatus. The entrance baffle and the main baffle form a two-stage fore baffle which are used to block stray light with an off-axis Angle greater than 20° outside the field of view. The baffle vanes are also designed according to the two-reflect design law, which requires the incident light to be reflected two times before reaching the PM.

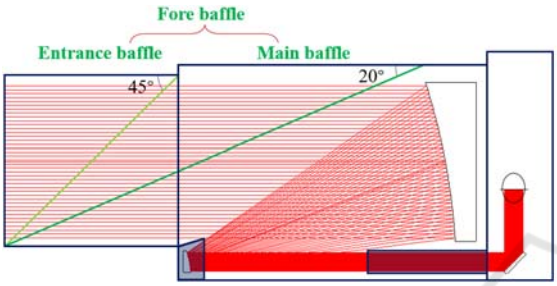

Figure 4: Two-stage structure layout of the fore baffle.

3.2 Array Design of Inner Baffle

The auxiliary coordinate points needed in the design of the inner baffle array in the three-aperture off-axis imaging system are shown in Figure 5. Point O is the intersection point between the rotational symmetry axis of the compact off-axis transmission system and the backplane of the primary mirror, which is set as the coordinate origin of the whole system. The plane of the backplane of the primary mirror is the XOY plane, and the plane perpendicular to the backplate of the primary mirror points to the incident direction of the beam is Z-axis direction. Based on this, the right-handed coordinate system is established. O_A、O_B、O_C is the intersection of the optical axis of the off-axis transmission system of each sub aperture and the primary mirror backplane, and is also the center origin of the cylindrical inner baffle of the off-axis beam combining system of each sub aperture. According to the relative position of the off-axis transmission system, its spatial coordinate is $O_A(x_1, y_1, 0); O_B(x_2, y_2, 0); O_C(x_3, y_3, 0)$. The three points A, B and C are respectively the lowest point of the oblique section edge of the inner baffle in each sub-aperture off-axis beam transmission system, which is determined by the optical structure of the off-axis beam system, and their spatial position coordinates are $A(x_a, y_a, z_a); B(x_b, y_b, z_b); C(x_c, y_c, z_c)$. D, E and F are the edge points of the entrance baffle of the off-axis beam transmission system of each sub-aperture, which are determined by the optical structure and system size of the off-axis beam transmission system, and their spatial position coordinates are $D(x_d, y_d, z_d); E(x_e, y_e, z_e); F(x_f, y_f, z_f)$. Three points G, H and I are respectively the highest points of the oblique section edge of the inner baffle in the off-axis beam transmission system of each sub-aperture, and their spatial position coordinates can be obtained by the design method of the inner baffle array of the compact off-axis beam transmission system. Figure 6 shows the meridional profile of a single sub-aperture off-axis beam transmission system, from which the position of the central origin O_A of the cylindrical inner baffle of the sub-aperture off-axis beam transmission system can be defined. The position of the lowest point A at the edge of the oblique section of the baffle in the sub-aperture off-axis beam transmission system; The position of edge point D of the entrance baffle of the sub-aperture off-axis beam transmission system; And the position of the highest point G of the oblique section edge of the inner baffle of the sub-aperture off-axis beam transmission system can be successively determined.

The spatial position coordinates of three points G, H and I at the aperture edge of the inner baffle of the off-axis beam transmission system of each sub-aperture are solved as follows:

a. Solve the plane normal vector by using the basic method of space vector operation:

$$\overrightarrow{AB} = (x_b - x_a, y_b - y_a, z_b - z_a) = (a_1, b_1, c_1) \quad (1)$$

$$\overrightarrow{AF} = (x_f - x_a, y_f - y_a, z_f - z_a) = (a_2, b_2, c_2) \quad (2)$$

$$\overrightarrow{n_1} = \overrightarrow{AB} \times \overrightarrow{AF} = (b_1c_2 - b_2c_1, c_1a_2 - a_1c_2, a_1b_2 - a_2b_1) = (A_1, B_1, C_1) \quad (3)$$

In the above equation, $\overrightarrow{n_1}$ is the normal vector of the plane determined by three points of ABF. Similarly, the normal vector of the plane determined by three points of ACF is $\overrightarrow{n_2} = (A_2, B_2, C_2)$, and the normal vector of the plane determined by three points of BCD is $\overrightarrow{n_3} = (A_3, B_3, C_3)$.

Furthermore, using the basic method of spatial analytic geometry, the following plane equation is obtained:

The plane equation determined by the three points of ABF is:

$$A_1(x-x_a)+B_1(y-y_a)+C_1(z-z_a)=0 \quad (4)$$

The plane equation determined by the three points of ACE is:

$$A_2(x-x_c)+B_2(y-y_c)+C_2(z-z_c)=0 \quad (5)$$

The plane equation determined by the three points of BCD is:

$$A_3(x-x_b)+B_3(y-y_b)+C_3(z-z_b)=0 \quad (6)$$

b. According to the known coordinate positions of space points, the following surface equations are obtained by using the basic method of spatial analytic geometry:

The equation of cylindrical surface of the inner baffle of the sub-aperture off-axis beam transmission system with O_A as the central origin is:

$$(x-x_1)^2+(y-y_1)^2 = (x_a-x_1)^2+(y_a-y_1)^2=R_1^2 \quad (7)$$

In the above equation, R_1 is the radius of the cylindrical inner baffle of the sub-aperture off-axis beam transmission system with O_A as the center of the circle.

In the same way, the equation of cylindrical surface of the inner baffle of the sub-aperture off-axis beam transmission system with O_B as the central origin is:

$$(x-x_2)^2+\left(y-y_2\right)^2 = (x_b-x_2)^2+(y_b-y_2)^2=R_2^2 \quad (8)$$

In the above equation, R_2 is the radius of the cylindrical inner baffle of the sub-aperture off-axis beam transmission system with O_B as the center of the circle.

The equation of cylindrical surface of the inner baffle of the sub-aperture off-axis beam transmission system with $O_C$as the central origin is:

$$(x-x_3)^2+(y-y_3)^2 = (x_c-x_3)^2+(y_c-y_3)^2=R_3^2 \quad (9)$$

In the above equation, R_3 is the radius of the cylindrical inner baffle of the sub-aperture off-axis beam transmission system with O_C as the center of the circle.

c. The intersection line is obtained by intersecting the pairwise plane. The intersection line intersects the cylindrical surface of a single sub-aperture off-axis beam transmission system to obtain the spatial position coordinates of the highest point and lowest point of the oblique section edge of the inner baffle in the sub-aperture off-axis beam transmission system.

The lowest point $A(x_a, y_a, z_a)$ and the highest point $G(x_g, y_g, z_g)$ at the edge of the cylindrical inner shading tube of the sub-aperture off-axis beam system with O_A as the center origin are obtained by solving equations (1), (2) and (4).

The lowest point $B(x_b, y_b, z_b)$ and the highest point $H(x_h, y_h, z_h)$ at the edge of the cylindrical inner shading tube of the sub-aperture off-axis beam system with O_B as the center origin are obtained by solving equations (1), (3) and (5).

The lowest point $C(x_c, y_c, z_c)$ and the highest point $I(x_i, y_i, z_i)$ at the edge of the cylindrical inner shading tube of the sub-aperture off-axis beam system with O_C as the center origin are obtained by solving equations (2), (3) and (6).

d. After obtaining the highest point and lowest point of the cylindrical surface edge of the inner baffle in the off-axis beam transmission system with a single sub-aperture, the inclination Angle θ of the oblique section of the inner baffle of the off-axis beam transmission system is solved according to the basic method of space vector calculation.

As shown in Figure 7, one end of the inner baffle of a single sub-aperture off-axis beam transmission system is plane and fixed on the backplane of the off-axis primary mirror. The other end is inclined section, which angle with the normal unit vector $\vec{N}=(0,\ 0,\ 1)$ of the backplane of the primary mirror is θ.

$\overrightarrow{AG}=\left(x_g-x_a, y_g-y_a, z_g-z_a\right)$ is the vector in the oblique section plane of the cylindrical inner baffle of the off-axis beam transmission system of the sub-aperture which central origin is O_A, then the inclined angle of the inclined section,

$$\theta_1=\arccos\frac{\overrightarrow{AG}\cdot\vec{N}}{\left|\overrightarrow{AG}\right|\cdot\left|\vec{N}\right|} \quad (10)$$

$\overrightarrow{BH}=(x_b-x_h, y_b-y_h, z_b-z_h)$ is the vector in the oblique section plane of the cylindrical inner baffle of the off-axis beam transmission system of the sub-aperture which central origin is O_B, then the inclined angle of the inclined section,

$$\theta_2=\arccos\frac{\overrightarrow{BH}\cdot\vec{N}}{\left|\overrightarrow{BH}\right|\cdot\left|\vec{N}\right|} \quad (11)$$

$\overrightarrow{CI}=(x_c-x_i, y_c-y_i, z_c-z_i)$ is the vector in the oblique section plane of the cylindrical inner baffle of the off-axis beam transmission system of the sub-

aperture which central origin is O_C, then the inclined angle of the inclined section,

$$\theta_3 = \arccos\frac{\overrightarrow{CI}\cdot\vec{N}}{|\overrightarrow{CI}|\cdot|\vec{N}|} \quad (12)$$

e. In the multi-aperture off-axis beam transmission system, the inclined section of the inner baffle which center is O_A is perpendicular to the plane determined at three points AGO_A. And the angle between it and the normal vector $\vec{N}$ of the backplane of primary mirror is θ_1.

In the multi-aperture off-axis beam transmission system, the inclined section of the inner baffle which center is O_B is perpendicular to the plane determined at three points BHO_B. And the angle between it and the normal vector $\vec{N}$ of the backplane of primary mirror is θ_2.

In the multi-aperture off-axis beam transmission system, the inclined section of the inner baffle which center is O_C is perpendicular to the plane determined at three pointsCIO_C. And the angle between it and the normal vector $\vec{N}$ of the backplane of primary mirror is θ_3.

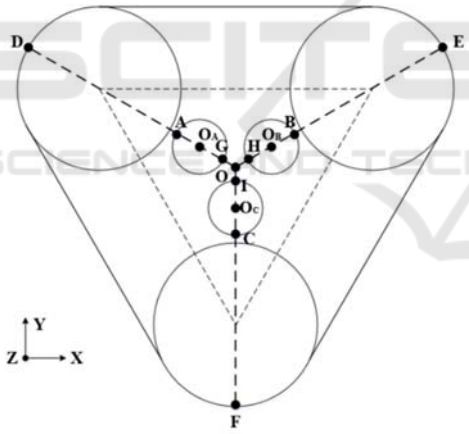

Figure 5: Key point indicator diagram.

In the 3D modeling software, according to the above spatial position relationship and the angle θ_1、θ_2、θ_3 of the inclined section calculated in Step 4, the inner baffle array of the compact multi-aperture off-axis beam transmission system can be easily and quickly established. The inner baffle array of the compact three-aperture off-axis beam transmission system is shown in Figure 8. Compared with the three-aperture off-axis beam transmission system with flat port as shown in Figure 9, the oblique structure of the inner baffle array is more reasonable. Under the condition of not blocking the imaging light of the system, the shading range of the inner baffle array to stray light outside the view field is fully increased.

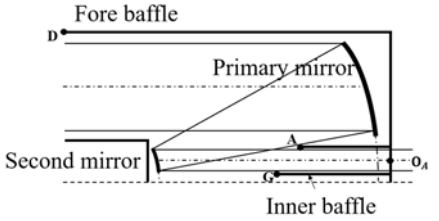

Figure 6: Auxiliary coordinate point indication diagram.

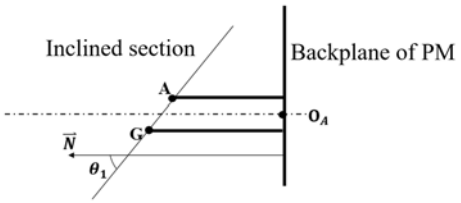

Figure 7: Meridional profile of a single sub-aperture off-axis beam transmission system.

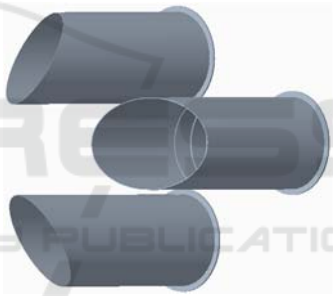

Figure 8: Inclined section inner baffle array.

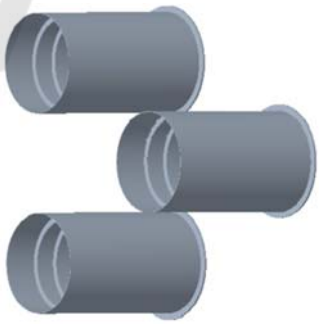

Figure 9: Flush inner baffle array.

4 BLACK BAFFLE SURFACE MEASUREMENT

Optical instruments and telescopes rely on black baffle and vane surfaces to minimize the effect of

stray light on overall system performance. For well-designed and well-baffled systems, the black surfaces chosen for the baffles and vanes can play a significant role in reducing the stray light on the detector. Space-based surfaces must withstand severe launch vibrations, temperature extremes, collisions with space debris and micrometeoroids, and exposure to ultraviolet radiation.

Taking into account the environmental adaptability and structural rigidity of the baffle, we measured the surface scattering characteristics of samples of four materials: inorganic anodized Al/SiC, anodized TC4, and untreated CFRP, anodized invar steel. Modular Light Scattering System (MLS 5) was used as the test equipment, as shown in Figure 10. Laser has high brightness, good directivity and high stability, which makes it a conventional light source for optical scattering measurements. The laser illuminates the sample surface to generate scattered light, and the detector with pinhole solid angle receives the scattered light energy of different scattering angles. The scattering measurement curves of the four sample surfaces are shown in Figure 11.

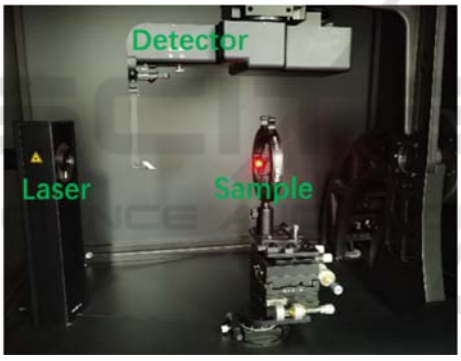

Figure 10: The BRDF measurement scene.

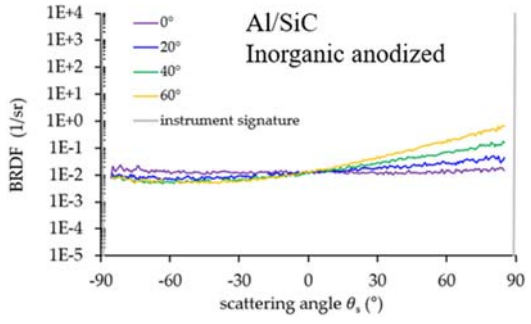

(a)

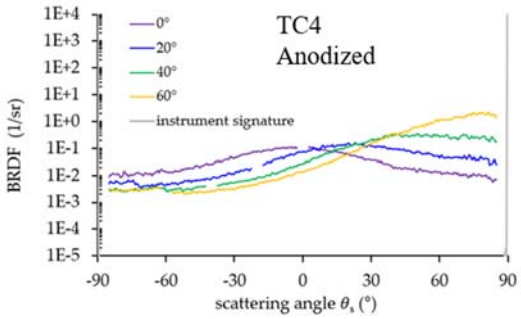

(b)

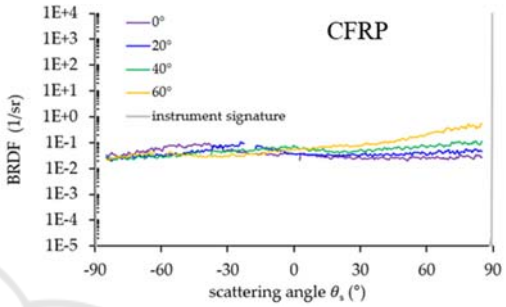

(c)

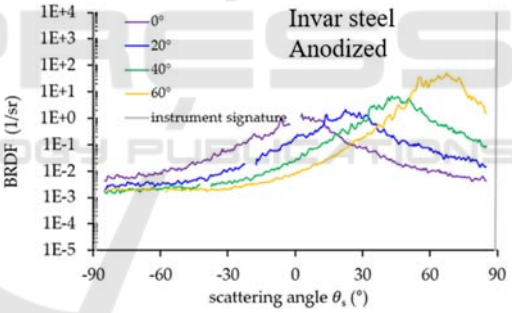

(d)

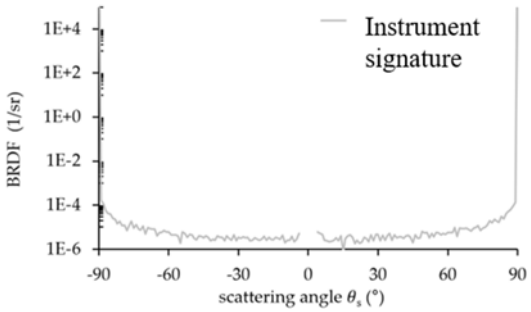

(e)

Figure 11: Measured BRDF data for sample (a) Al/SiC inorganic anodized (b) TC 4 anodized (c) CFRP (d) Invar steel anodized (e) instrument signature for a scan along to the plane of incidence.

According to the measured data, it can be seen that the BRDF of inorganic anodized Al/SiC and untreated CFRP is small, followed by anodized TC4 and anodized invar steel is the largest. Considering the processing performance and cost performance of the materials, etc., finally, CFRP was selected as the baffle material for the compact multi-aperture imaging instrument.

5 SIMULATION ANALYSIS

The measured CFRP surface scattering data are brought into the surface property editor module of Tracepro, a stray light analysis software. The measured surface property is assigned to the mask model. The off-axis angle range of the stray light is 18°-28°, where the out of field stray light incident from the adjacent aperture can directly through the back plate of the primary mirror, and shine on the 45 ° mirror. We analyzed the PST of the system within this off-axis angle range, and the curve obtained by simulation analysis is shown in Figure 12. The red curve in the Figure shows the PST data of the model simulation with the inclined section inner baffle array. The blue curve in the Figure shows the PST data of the model simulation with the flush section inner baffle array. It can be seen from the curve in the Figure that although the PST values of model with the in inclined section inner baffle array have some fluctuations, they are all three orders of magnitude smaller. It can be explained that the proposed method can effectively improve the cross-talk of external stray light between the sub-aperture of the multi-aperture off-axis beam transmission system.

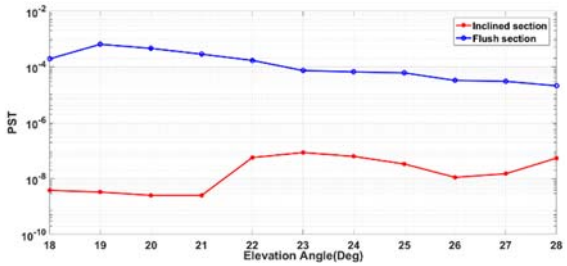

Figure 12: PST value between 18° and 28° off-axis angle.

6 CONCLUSION

In this paper, a fast modeling method is designed for a compact multi-aperture off-axis imaging system, and an opto-mechanical model equipped with a two-stage fore baffle and an inner baffle array is designed by taking the compact three-aperture off-axis imaging system as an example. The BRDF data of anodized Al/SiC, anodized TC4, untreated CFRP and anodized invar steel were tested by scatterometer. Finally choose untreated CFRP with the highest cost performance as the material of the baffle. The surface attribute editing function in the stray light analysis software was used to bring the actual measured BRDF data into the opto-mechanical model, and the PST of the inclined section and the flush section of the inner baffle array were simulated and calculated respectively. The analysis results show that the proposed method can effectively improve the cross-talk of external stray light between the sub-aperture of the multi-aperture off-axis beam transmission system.

ACKNOWLEDGEMENTS

J. L. Guo, M. L. Zhang, thanks for providing mechanical structure models for the analyses.

REFERENCES

E. C. Fest, (2013) *Stray Light Analysis and Control*, SPIE Press, Bellingham, Washington .

M. Asadnezhad, A. Eslamimajd, H. Hajghassem, H. Hajghassem. (2018) *Stray light analysis, baffle, and optical design of a high-resolution satellite camera*. J. Appl. Remote Sens. 12, 026009.

C. Leinert, D. Kluppelberg. (1974) *Stray light suppression in optical space experiments*. Appl. Opt., 13, 556-564 .

W. L. Hales. (1992) *Optimum Cassegrain baffle systems*, Appl. Opt. 31, 5341–5344 .

M. S. Kumar, C. Narayanamurthy, and A. K. Kumar. (2013) *Iterative method of baffle design for modified Ritchey-Chretien telescope*, Appl. Opt. 52, 1240–1247 .

S. M. Pompea and R. P. Breault. (1995) *Black surfaces for optical systems*, in Handbook of Optics, M. Bass, Ed., 2nd ed., 2, 37.31-37.63 (1995).

Peixian Han, JunliGuo. (2021) *Optical design and stray light control for the space-based laser space debris removal mission*, Appl. Opt. 2021, 60(25):7721-7730.